



Long-lifetime spin excitations near domain walls in 1T-TaS₂

Anuva Aishwarya^{a,b}, Arjun Raghavan^{a,b}, Sean Howard^{a,b}, Zhuozhen Cai^{a,b}, Gohil S. Thakur^{c,d}, Choongjae Won^{e,f}, Sang-Wook Cheong^{e,f,g,h}, Claudia Felser^c, and Vidya Madhavan^{a,b,1}

Edited by Ali Yazdani, Princeton University, Princeton, NJ; received December 7, 2021; accepted April 8, 2022

Spin chains in solid state materials are quintessential quantum systems with potential applications in spin-based logic, memory, quantum communication, and computation. A critical challenge is the experimental determination of spin lifetimes with the ultimate goal of increasing it. Local measurements by scanning tunneling microscopy (STM) have demonstrated the importance of decoupling spins from their environment, with markedly improved lifetimes in spin chains on the surfaces of band insulators. In this work we use low-temperature scanning tunneling microscopy to reveal long-lifetime excitations in a chain of spin-1/2 electrons embedded in a charge density wave Mott insulator, 1T-TaS₂. Naturally occurring domain walls trap chains of localized spin-1/2 electrons in nearby sites, whose energies lie inside the Mott gap. Spin-polarized measurements on these sites show distinct two-level switching noise, as well as negative differential resistance in the dI/dV spectra, typically associated with spin fluctuations. The excitations show exceptionally long lifetimes of a few seconds at 300 mK. Our work suggests that layered Mott insulators in the chalcogenide family, which are amenable to exfoliation and lithography, may provide a viable platform for quantum applications.

spin chain | scanning tunneling microscopy | noise spectroscopy

Spin chains in one dimension (1D) have been used as prototypical systems to study quantum mechanical phenomena in lower dimensions due to their simplicity, integrability, and scalability. Their 1D nature can enhance correlation effects leading to exotic quasiparticle excitations due to spin-charge separation (1, 2), as well as Majorana edge states (3, 4) when coupled to a superconductor. One-dimensional spin chains thus provide a fertile playground for realizing new states of matter at the intersection of strong correlations, magnetism, topology, and superconductivity. Scanning tunneling microscopy and spectroscopy (STM/S) have provided unprecedented access and control at the atomic scale for the study of 1D spin chains compared to other ensemble averaging techniques like angle-resolved photoemission spectroscopy, neutron scattering, or magnetic susceptibility. Properties such as spin lifetimes, spin order, and the energetics of 1D spin chains have been explored in great detail using STM-based atomic manipulation (5-15). These studies have established that the substrate harboring the spin chain can affect the ground state configuration, spin-spin interactions, and the spin lifetimes dramatically (5). Long spin lifetimes have been observed on spin chains on insulating substrates and are highly desirable due to their applicability in quantum information technologies. More recently, optical studies of Mott insulating states in transition metal dichalcogenide moiré superlattices have shown unusually long spin lifetimes emerging from strong correlations (16). Mott insulators are therefore a new and unique platform to study spins in the presence of many-body interactions. In this work we use STM/S to probe the lifetime of quasi-1D spin chains trapped at the domain walls (DWs) in the layered Mott insulator, 1T-TaS₂.

The insulator 1T-TaS₂ is an intriguing system that undergoes a low-temperature transition into a charge density wave (CDW) Mott insulator without magnetic order. The commensurate CDW (CCDW) phase that emerges below 200 K has CDW clusters that resemble the famous Star of David (SD) shape. In this work, we study cleaved 1T-TaS₂ single crystals measured at temperatures between 300 mK and 14 K. Fig. 1A shows a schematic of the CDW. Each SD cluster in the CDW phase consists of 12 Ta outer atoms on the SD that move toward a center Ta atom, giving a total of 13 Ta atoms per SD cluster. The SDs form a triangular lattice which is $\sqrt{13} \times \sqrt{13}$ times larger than the unreconstructed lattice (17). Fig. 1B shows an STM image of a large area where each protrusion represents an SD cluster with Fig. 1 B, Inset, showing a high-resolution image of the reconstructed S atoms (white dotted lines).

The CDW transition is accompanied by a metal-insulator Mott transition (18) which results in the occupation of a single unpaired electron per cluster that occupies a narrow Hubbard band below the Fermi energy. This picture comes from the wellunderstood band structure and charge arrangement in the insulating phase, as we describe here. Each of the 13 Ta⁴⁺ sites in the cluster has one 5d electron (19). With

Significance

There is an intense ongoing search for two-level quantum systems with long lifetimes for applications in quantum communication and computation. Much research has been focused on studying isolated spins in semiconductors or band insulators. Mott insulators provide an interesting alternative platform but have been far less explored. In this work we use a technique capable of resolving individual spins at atomic length scales, to measure the two-level switching of spin states in 1T-TaS2. We find quasi-1D chains of spin-1/2 electrons embedded in 1T-TaS₂ which have exceptionally long lifetimes. The discovery of longlived spin states in a tractable van der Waal material opens doors to using Mott systems in future quantum information applications.

Author contributions: A.A. and V.M. designed research; A.A., A.R., S.H., and Z.C. performed research; A.A., A.R., G.S.T., C.W., S.-W.C., and C.F. contributed new reagents/ analytic tools; A.A. analyzed data; and A.A. and V.M. wrote the paper.

The authors declare no competing interest.

This article is a PNAS Direct Submission.

Copyright © 2022 the Author(s). Published by PNAS. This article is distributed under Creative Commons Attribution-NonCommercial-NoDerivatives License 4.0 (CC BY-NC-ND).

¹To whom correspondence may be addressed. Email:

This article contains supporting information online at http://www.pnas.org/lookup/suppl/doi:10.1073/pnas. 2121740119/-/DCSupplemental.

Published May 26, 2022.

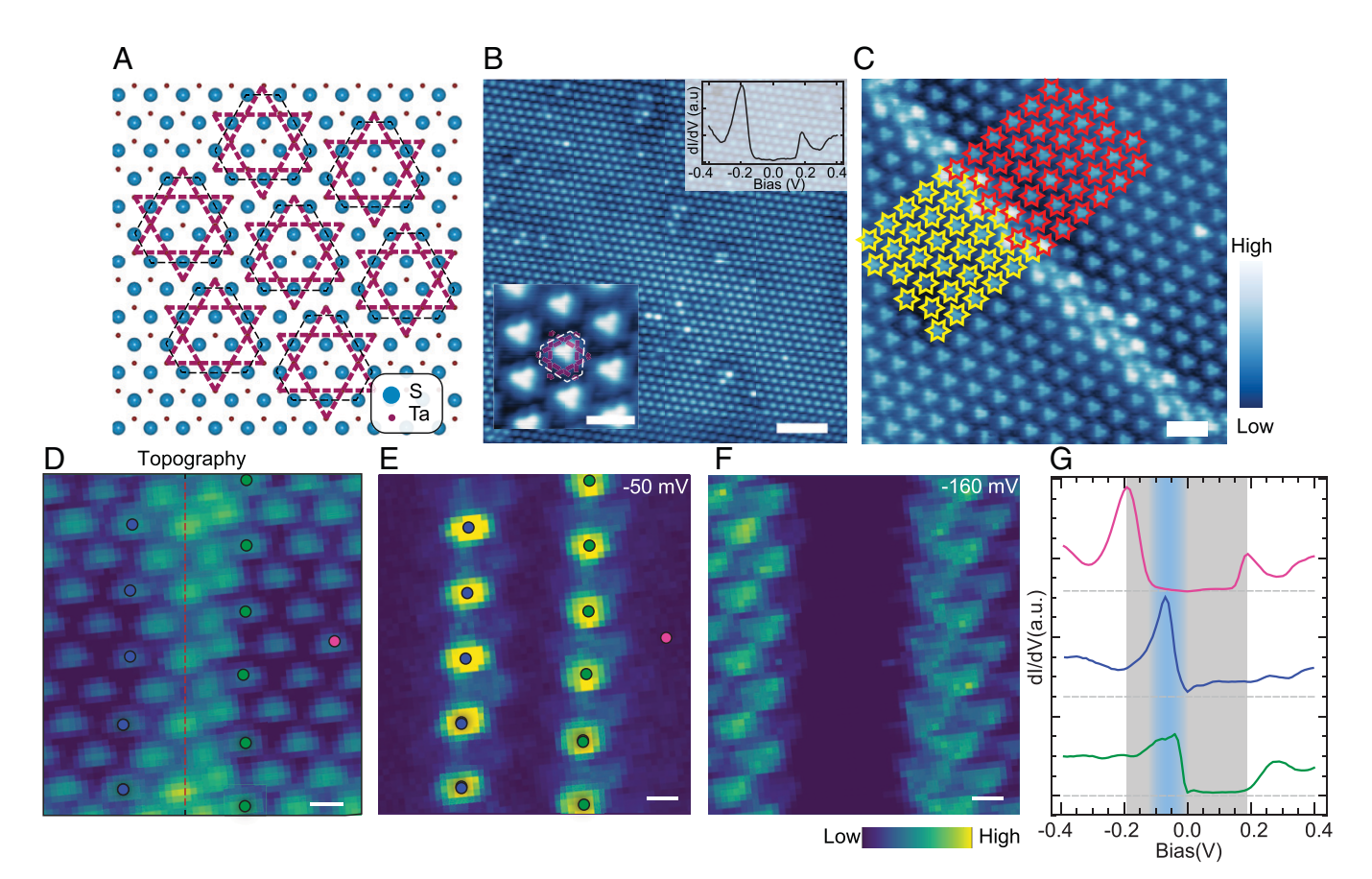


Fig. 1. CDW DW in 1T-TaS₂: structure, morphology, and localized quasi-1D electrons near the DW. (A) Schematic of the SD reconstruction in monolayer TaS_2 showing the positions of the tantalum (smaller purple dots) and sulfur (blue dots) atoms. (B) Large area STM topography (50 nm \times 50 nm) showing the $\sqrt{13} \times \sqrt{13}$ reconstructed surface (V_S = 300 mV, I_t = 30 pA). (Scale bar, 5 nm.) (Bottom Inset) A zoomed in view of the reconstructed lattice with the SD overlay. (Scale bar, 1 nm.) (Top Inset) Typical dI/dV spectrum far from DWs. The two peaks around ±0.2 eV are associated with the UHB and LHB, respectively. (C) STM topography (18 nm × 18 nm) of an area with the DW studied in this work. The SD clusters on the two sides of the DW are marked in yellow and red (V_{bias} = 400 mV, $I_t = 40 \text{ pA}$). (Scale bar, 5 nm.) (D) Topography obtained simultaneously with the LDOS maps on a DW. Green/blue circles show the location of the localized spins. (E) LDOS map at -50 mV. The green/blue colored dots label the location of the localized low-energy electrons. (F) LDOS map at -160 mV (close to the energy of the LHB). The dark area reflects a suppression of the DOS due to band bending. (Scale bar in D-F, 1 nm.) (G) dI/dV spectra obtained on the localized electron sites (blue and green dots in E) and a far-off site (pink). The spectra shown are averaged over similar sites. The shaded gray area $denotes \ the \ Mott \ gap. \ The \ shaded \ blue \ area \ denotes \ the \ energy \ of \ the \ localized \ electrons \ inside \ the \ Mott \ gap.$

an odd number of electrons per cluster, band theory would predict that 1T-TaS2 should be a metal. However, 1T-TaS2 is instead an insulator (19, 20). Density functional theory calculations attribute this to the occurrence of a narrow, flat band that crosses the Fermi energy (E_F) in the CCDW state, which splits into upper and lower Hubbard bands (UHB and LHB) due to a correlation-driven Mott transition (21). The Hubbard bands are located symmetrically about E_F at $\pm\,200$ meV inside the CDW gap (± 300 meV), as shown in Fig. 1 B, Inset. We note that the LHB hosts only one electron per cluster, with the remaining electrons occupying a multiplicity of d bands several hundred meV below E_F (18, 21). While the existence of a single unpaired spin per cluster would normally suggest an antiferromagnetic ground state, no magnetic ordering has been observed even at the lowest temperatures, and a quantum spin liquid picture has been proposed to explain the absence of ordering (22).

A Mott insulator with a well-defined bulk gap and one unpaired spin per site is an ideal candidate to study the behavior of localized spins. Kondo physics has been observed, for example, in a similar CDW Mott insulator in proximity to a metal (23). Interestingly, previous STM studies have shown that the local potential generated by CDW DWs in 1T-TaS₂ can cause an energy shift of the bands as one approaches the DW (24-28) and trap localized charge. Fig. 1 C and D show

an image of one such DW. As shown in Fig. 1G and SI Appendix, Fig. S1, the DW potential causes the energies of the UHB and LHB to shift as we move closer to the DW from either side and creates a quasi-1D potential trap for electrons. Fig. 1 E and F show STM dI/dV maps (or local density of states [LDOS] maps) in the vicinity of the DW. As shown in Fig. 1E, the low-energy LDOS map within the bulk Mott gap reveals a pattern of bright clusters localized on two rows of SD sites on either side of the DW. This can also be seen in the integrated density of states inside the Mott gap (SI Appendix, Fig. S2).

We thus find that the low-energy occupied states near the DW are localized to two rows of SD clusters (marked by blue/ green dots in Fig. 1 D and E and SI Appendix, Fig. S2) on either side of the DW, aligned in a quasi-1D pattern (henceforth dubbed "quasi-1D chains"). As marked by the blue/green dots in Fig. 1D, the quasi-1D chains are not at the DW itself but are at nearby locations, at a distance of ~1.5 nm from the DW. A combination of correlation effects, broken rotational and translational symmetry near the DW, and the strong potential provided by the SD clusters likely causes this charge localization. These trapped electrons in the quasi-1D chains are both energetically and spatially decoupled from the surrounding lattice as shown schematically in Fig. 2B. In the bulk (i.e., far from the DW), each SD cluster is known to host one spin-

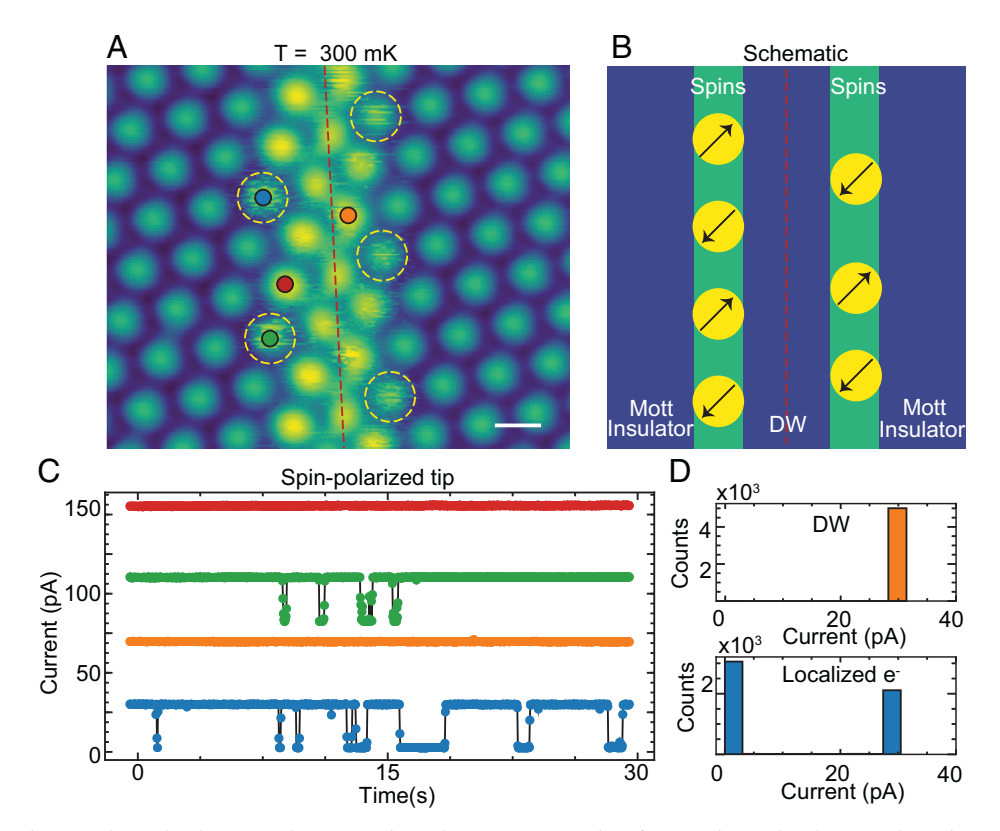


Fig. 2. Quasi-1D spin chains with two-level noise with a spin-polarized tip. (A) Topography of a DW obtained with spin-polarized tip at 300 mK. (Scale bar, 1 nm.) (B) Schematic of the electrons/spin chains along the DW inside the Mott gap. The red dashed line depicts the position of the DW. (C) Noise measurements, i.e., time traces of the tunnel current, obtained on the marked sites (as indicated in A). The time traces have been color-referenced to the clusters they were obtained on. The sweeps are offset by 30 pA for clarity. The blue and green sweeps show the presence of two-level telegraph noise on the SD cluster near the DW and an absence of it on the DW. The measurements were made with a spin-polarized tip, tunnel current $I_t = 30$ pA, and $V_{Bias} = 30$ mV with the feedback loop turned off. (D) The histogram plots of the current sweeps show a two-level distribution for the blue site (which is absent for the DW site).

1/2 electron at the energy of the LHB which is ~200 meV below E_F. Near the DW, the energies of these electrons are shifted such that they fall inside the bulk insulating gap (Fig. 1G), causing them to be energetically decoupled from the surrounding clusters. The spatial decoupling can be seen in LDOS maps below the E_F. Nearby clusters on either side of the quasi-1D chains are not occupied at these energies (also see SI Appendix, Fig. S2). The quasi-1D chains are thus able to act as a subsystem within an insulator, mimicking a chain of spin-1/2 electrons (Fig. 2B). Free from the frustration of the bulk triangular lattice, and given the typical antiferromagnetic correlations in Mott systems, these sites may exhibit short-range spin order.

We next characterize this quasi-1D chain with spin-polarized STM. The spin sensitivity of the Cr tips was confirmed by imaging the antiferromagnetic stripes on FeTe (SI Appendix, Fig. S3). Our most striking finding is the existence of switching noise, which is localized to the clusters on the quasi-1D chain. This noise is visible in the current channel as shown in Fig. 2C and can be captured by noise spectroscopy, i.e., a measurement of the tunneling current as a function of time [I(t)] with the feedback off. From Fig. 2C (and SI Appendix, Figs. S4-S6) we see that the I(t) on the clusters making up the quasi-1D chain shows noise with characteristics of two-level switching with a time scale of the order of a few seconds at 300 mK. This is exemplified by the histogram of the current values which displays a bimodal distribution characteristic of the two-level behavior (see Fig. 2D and SI Appendix, Fig. S6, for better statistics).

This immediately leads to the question of what might be responsible for this long-lifetime two-level switching. First, we can easily rule out tip effects as the source: the noise is site dependent and occurs on specific clusters (green dots in Fig. 2A; also see SI Appendix, Fig. S4). We have confirmed the same phenomenology with 11 different tips on eight different samples on more than 50 DWs. Second, we can rule out structural fluctuations of the DW. In fact, the clusters nearest to the DW show far less or negligible noise as shown in Fig. 2C.

A critical hint to the origin of the switching noise is obtained by comparing our exceptionally long lifetimes to earlier STM experiments on chains of coupled spins arranged on a substrate through atomic manipulation. Several studies have been performed on such systems, and it is known that they show twolevel noise with similar slow time scales (order of 100 ms or more) (8-12, 15). This suggests that the noise may arise from spin excitations. To further explore the possibility that spin flips are the source of the switching noise, we compare dI/dV spectra obtained with normal (W tips) and spin-polarized tips (Cr tips). Previous studies have shown that noise related to spin configuration changes is characterized by an inelastic signal in dI/dV spectra obtained with a normal tip (refs. 6, 7 and supplement of ref. 8) and a corresponding negative differential conductance (NDC) signal in dI/dV measured with a spin-polarized tip (30).

We first examine dI/dV spectra obtained with a normal tip. An inelastic signal is observed when tunneling electrons excite a bosonic mode, and the signature is a step-like increase in the dI/dV spectrum at the energy of the mode. The energy scale of the inelastic modes measured by previous STM studies on magnetic clusters and antiferromagnetic spin chains is typically a few meV to few tens of meV (refs. 6, 7 and supplement of ref. 8). In our system, we observe a clear inelastic signal on the SD clusters near the DWs that are seen as steps in the tunnel

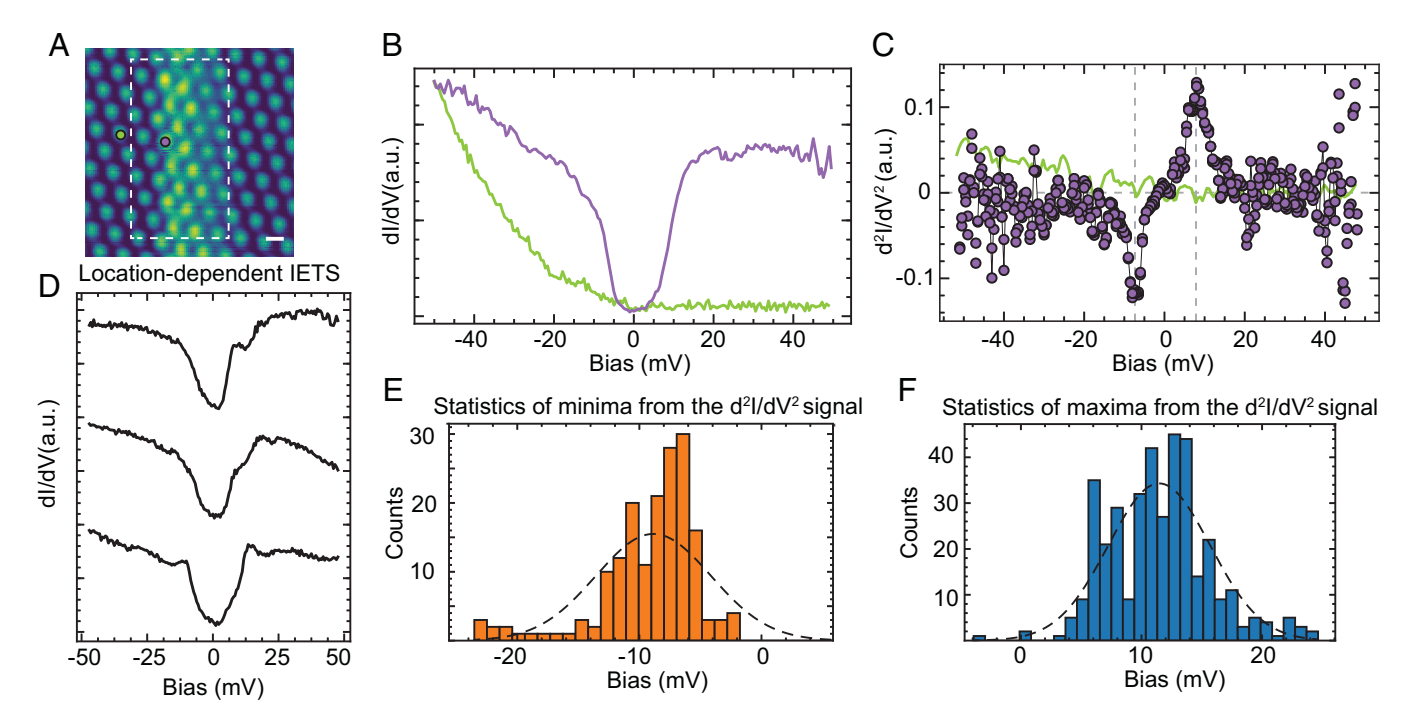


Fig. 3. Inelastic electron tunneling spectroscopy (IETS) signal in the dI/dV spectra at 300 mK obtained with a W-tip. (A) Topography of the DW showing clusters where the noise or dI/dV spectra in B were obtained. (Scale bar, 1 nm.) (B) dI/dV spectrum obtained on cluster with noise showing an inelastic signal $(V_{bias} = 50 \text{ mV}, I_t = 50 \text{ pA})$ (purple). dI/dV spectrum on a nearby cluster without noise which also does not show an inelastic signal. $(V_{bias} = -70 \text{ mV}, I_t = 50 \text{ pA})$ pA) (green). (C) Derivative of the dl/dV signals showing the symmetric peak-dip feature at the energies associated with the inelastic mode (purple) but a featureless signal for the green curve. (D) IETS of different energies obtained at different locations near the DW shown in C. (E and F) Histogram of the energies of the peaks and dips of d^2I/dV^2 , respectively, obtained around the DW shown by the dotted rectangle in A. The fitted Gaussian shows that the IETS signals at different locations near the DW follow a distribution around a mean value of 11 meV.

current on either side of the Fermi energy. These inelastic signatures are absent in spectra on neighboring clusters as well as in the bulk (Fig. 3B and SI Appendix, Fig. S7). The energy of these excitations can be determined by looking at the peakdip energies in the derivative of the dI/dV signal (d^2I/dV^2) ; Fig. 3C). In an antiferromagnetic spin chain the energy of the onset of the inelastic signal is a measure of J, the antiferromagnetic exchange interaction (or Heisenberg coupling). A statistical

analysis of the inelastic mode energies as determined by the peak and dip values near one particular DW is shown as a histogram in Fig. 3 E and F. The mean mode energy for this DW is 11 meV, which is a similar order of magnitude compared to the previous studies on spin chains. We also find that the type and length of DWs have an effect on the average inelastic mode energy (SI Appendix, Fig. S8). This is expected since the details of the DW potential, length, and anisotropy in the exchange

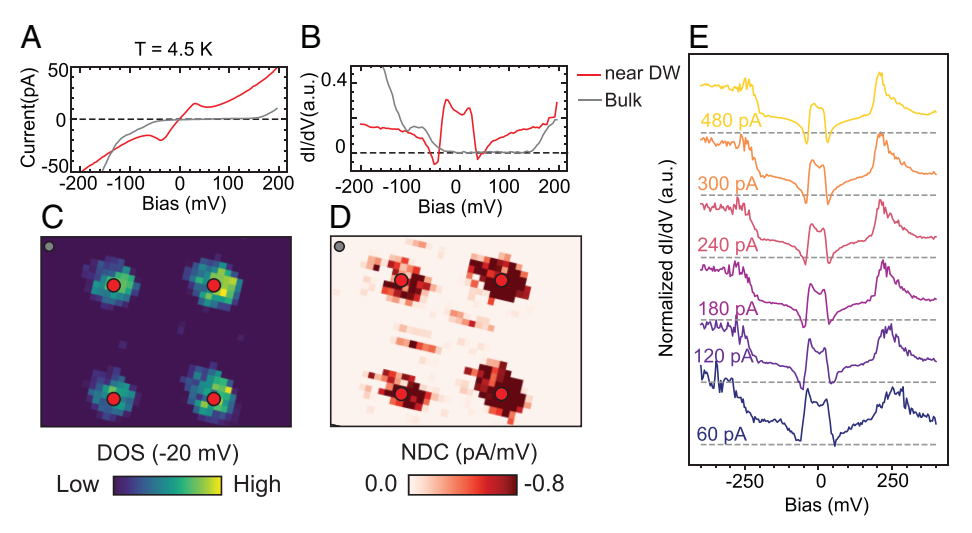


Fig. 4. Spin-based NDC on the trapped electron sites measured with a spin-polarized tip. (A) Tunnel current obtained with a spin-polarized tip as a function of bias showing NDC at low energies near a DW. The locations of the spectra are indicated by gray and red circles in C and D. (B) dl/dV spectrum corresponding to A. The NDC manifests as negative values of the dI/dV. (C) Density of states (LDOS) map near DW at -25 mV showing the trapped electrons. (D) NDC map obtained with a spin-polarized tip near DW. A strong correlation between position of the electrons and strong NDC below E_F is evident (the details of obtaining the NDC map are in SI Appendix). (E) Normalized dl/dV spectra as a function of set point tunneling current obtained with a spin-polarized tip. V_{Bias} = 400 mV. The spectra have been normalized at 400 mV. The gray dashed line indicates the zero conductance. The NDC is small when the tip is far away (60 pA) but becomes successively stronger as the tip is moved closer to the sample (480 pA).

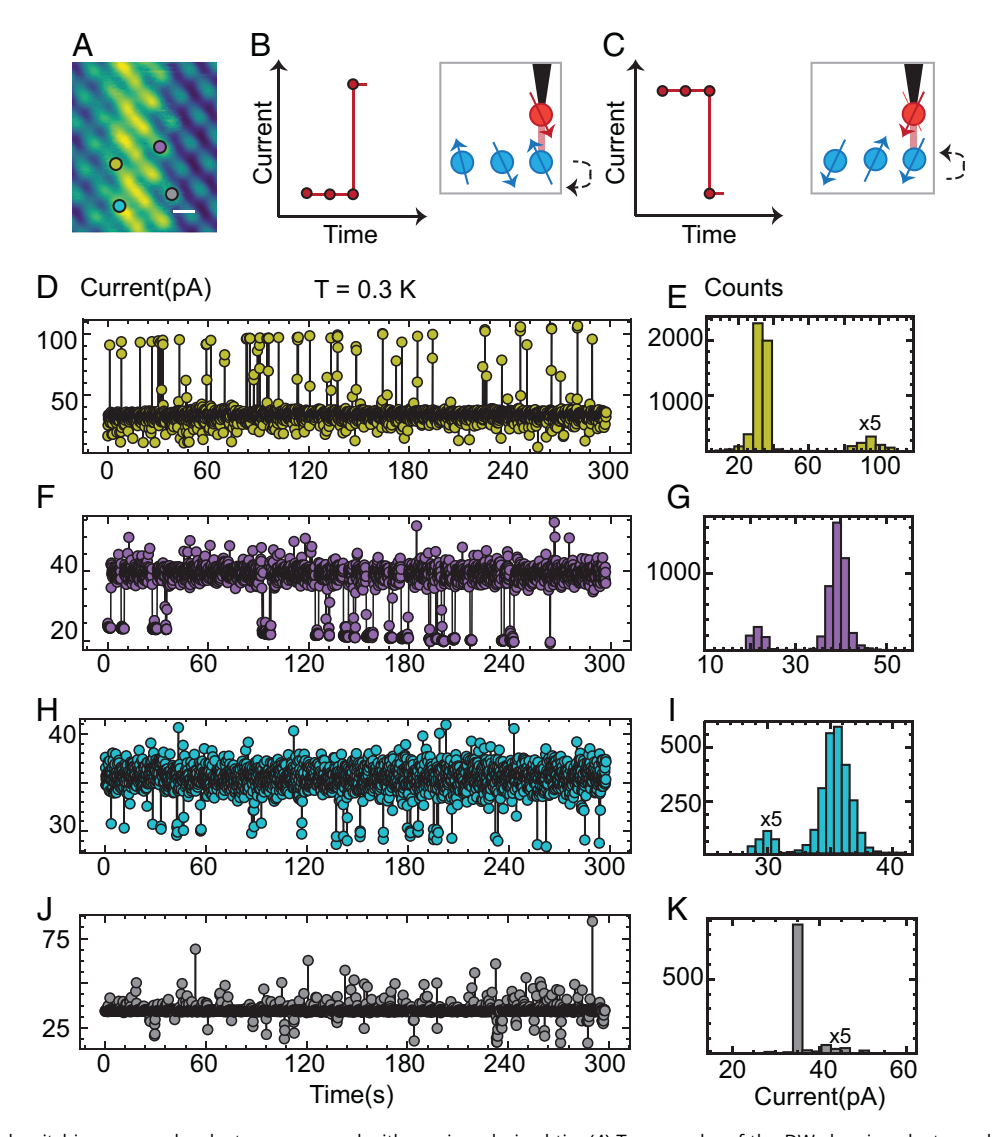


Fig. 5. Anticorrelated switching on nearby clusters measured with a spin-polarized tip. (A) Topography of the DW showing clusters where the noise spectra were obtained with the spin-polarized tip. (Scale bar, 1 nm.) (B and C) Schematic of the spin-polarized tunnel current when the spins flip from a state with a lower current to a higher current and vice versa. (D, F, H, and J) Current sweeps with feedback off obtained on clusters shown in C. All the sweeps were obtained at $V_{bias} = 30$ mV, $I_t = 30$ pA at T = 300 mK. A small linear background has been subtracted from all of them that occurs due to piezo relaxation when the feedback is turned off. D and J show current behavior similar to the scenario in B, and F and H show current behavior similar to the scenario in C. (E, G, I, and K) Histograms of the current sweeps that show anticorrelated switching behavior between the two states for neighboring clusters. E and G and I and K show pairwise anticorrelation between the occupation of the up and down states. In J, the switching rate is much lower compared to D, F, and H possibly because the spin is located farther from the other spins.

couplings at each site determine possible ground-state and excited-state spin configurations (7, 29).

We next measure dI/dV spectra with a spin-polarized tip. In previous STM studies on spin chains, normal tips show an inelastic signal, while spin-polarized tips show pronounced NDC (30). NDC refers to the phenomenon where the conductance (dI/dV) goes below zero for certain energies, signifying a decrease in tunnel current with increasing voltage. The NDC with spin-polarized tips was attributed to the tunneling electrons dynamically stabilizing an excited-state spin configuration (30). Observing NDC in this system is particularly important since the fluctuations smear out any static spin contrast. Fig. 4 A and B show I(V) and corresponding dI/dV on two different sites (marked in red/gray on the LDOS map in Fig. 4C). We find that the sites marked in red (corresponding to the clusters in the quasi-1D chain) show NDC with an energy scale comparable to inelastic excitations observed on similar DWs in our system. A spatial map of the NDC (see SI Appendix, Fig. S10,

for details) and a corresponding density of states map near a DW (Fig. 4 C and D) confirm that the NDC is sharply limited to the quasi-1D chain sites. Importantly, on moving the spinpolarized tip closer to the sample, the strength of NDC increases (Fig. 4E). This is as expected and demonstrates that the NDC is due to a coupling between the spin on the tip and the spins near the DW.

We have shown long-lived two-level switching noise in I(t), inelastic signal in dI/dV with normal tips, and NDC in dI/dV with spin-polarized tips, all centered on clusters in the quasi-1D chain. This phenomenology is very similar to previous STM measurements on artificial spin chains. Taken together this suggests that the two-level noise in our system originates from spin flip excitations. The question that remains is whether the spin flips correspond to local excitations of a spin-1/2 electron on a single cluster or whether our signal is from collective behavior.

Let us first consider the possibility that spin flips of the local spin on the cluster right under the tip are responsible for the observed switching noise. Earlier studies have shown that single spin flips of magnetic atoms may show long lifetimes (11) provided the spins involved are large (s = 2, for example). The spins in our case are expected to be spin-1/2, so individual spin flips are perhaps unlikely as the source of our noise. Another possibility is that the noise arises from coherent spin flips of the spin configuration of the chains (flipping of all spins from one direction to another for either ferromagnetically or antiferromagnetically coupled chains, for example). STM studies on different types of spin chains have shown that these occur at much slower time scales (8, 15). The antiferromagnetic exchange interaction in Mott insulators is given by $J \sim \frac{4t^2}{U}$, where U is the onsite repulsion and t is the bandwidth of the Hubbard band. Using $U\!\sim\!\!400~{\rm meV}$ and $t\sim\!\!70~{\rm meV}$ (from the measured $dI\!/dV$ spectrum) for 1T-TaS2, we get an estimate of O(10 meV) as the strength of the antiferromagnetic coupling between neighboring sites. Since the reduced symmetry of the low-energy electrons near the DW removes the frustration experienced by the local spins on the triangular lattice, it opens the possibility of shortrange antiferromagnetic ordering of the local moments. In this scenario, the noise behavior may be attributed to the excitation of the ground-state spin configuration to one or more excited-state spin configurations. While detailed theoretical studies are required to pin down the allowed spin ground and excited states in this system, a few possible configurations based on the geometry of the DWs are shown in SI Appendix, Fig. S11.

While the observed noise fluctuations prevent us from obtaining spin contrast of the spin chains through topography, we find that the two-level noise does provide information on the spin configuration. As shown schematically in Fig. 5 B and C, when the spin on the tip is aligned to the spin on the sample, a spin flip on the sample would reduce the net spin-polarized tunnel current (while an antiparallel initial configuration would lead to an increase in the current upon spin flip). Shown in Fig. 5 D, F, H, and J are the noise on neighboring sites on the spin chain obtained with the same set point. We find that neighboring sites (for, e.g., Fig. 5 D and H) preferentially go from a lower (higher) current state to a higher (lower) current state. The histograms in Fig. 5 E, G, I and K illustrate this finding. This anticorrelated behavior of the switching serves as an alternate route to observing the spin contrast of the chains. The observed antiferromagnetic correlation between the neighboring sites is compatible with the dominance of Mott physics in this system.

The noise characteristics, the inelastic signal, and the NDC with spin-polarized tips are all characteristic of behavior observed in 1D spin chains and leave us with compelling evidence that DWs in TaS₂ host locally ordered quasi-1D spin states with long lifetimes. Although the bulk of 1T-TaS₂ has no long-range order, defects like DWs can pin spins locally into a short-range ordered state. These long-lived spin states hold promise for integration into devices for future spintronics-based

- 1. T. Giamarchi, Quantum Physics in One Dimension (Clarendon, 2004).
- C. Kim et al., Observation of spin-charge separation in one-dimensional SrCuO₂. Phys. Rev. Lett. 77, 4054-4057 (1996).
- S. Nadj-Perge, I. K. Drozdov, B. A. Bernevig, A. Yazdani, Proposal for realizing Majorana fermions in chains of magnetic atoms on a superconductor. *Phys. Rev. B Condens. Matter Mater. Phys.* 88, 020407 (2013).
- S. Nadj-Perge et al., Topological matter. Observation of Majorana fermions in ferromagnetic atomic chains on a superconductor. Science 346, 602-607 (2014).
- D.-J. Choi et al., Colloquium: Atomic spin chains on surfaces. Rev. Mod. Phys. 91, 041001 (2019).
- S. Loth et al., Controlling the state of quantum spins with electric currents. Nat. Phys. 6, 340 (2010).
- C. F. Hirjibehedin, C. P. Lutz, A. J. Heinrich, Spin coupling in engineered atomic structures. Science 312, 1021–1024 (2006).
- S. Loth, S. Baumann, C. P. Lutz, D. M. Eigler, A. J. Heinrich, Bistability in atomic-scale antiferromagnets. Science 335, 196–199 (2012).

applications. Furthermore, strongly correlated spin chains in 1D are expected to exhibit spin–charge separation giving rise to quasiparticles such as spinons and chargons as have been observed in the quasi-1D Mott insulator SrCuO₂ (2). The DWs in TaS₂ have all the ingredients to exhibit spin–charge separation and could be prospective candidates to probe the existence of these exotic quasiparticles. Finally, rendering 1T-TaS₂ superconducting by gating or doping could provide another avenue to study spin chains coupled to a bulk superconductor and possible Majorana excitations.

Methods

High-quality 1T-TaS $_2$ crystals used in this study were obtained from two separate groups. Both batches show similar phenomenology. The experiments were performed in two Unisoku STMs with base temperatures 300 mK and 4.3 K unless stated otherwise. The single crystals were cleaved at ~ 90 K in ultra-high vacuum and immediately inserted into the STM. Spectroscopic measurements were performed by standard lock-in techniques. The spin-polarized tips were calibrated on Fe $_{1+x}$ Te, a known bicollinear antiferromagnet prior to their use. Noise spectroscopy was performed using a built-in module in the Nanonis package. The multigain preamplifier was set to a specific high frequency value (~ 1.1 kHz), and the sampling rate was controlled using the Nanonis module. The tip was placed over each cluster, and the current was recorded for a fixed amount of time.

Data Availability. All study data have been deposited in the Illinois Data Bank, https://databank.illinois.edu/datasets/IDB-0883774?code=gFz_9HQomnON51rNL1_Sr_Yc2Gil2XsYxADIuXwOEMg.

ACKNOWLEDGMENTS. The STM studies were primarily supported by the NSF Award DMR-2003784 and in part by the Gordon and Betty Moore Foundation's Emergent Phenomena in Quantum Systems Initiative (EPiQS), Grant GBMF9465. The work at Postech was supported by the National Research Foundation of Korea funded by the Ministry of Science and information and communications technology (Grant 2020M3H4A2084417). S.-W.C. is supported by the center for Quantum Materials Synthesis, funded by the Gordon and Betty Moore Foundation's EPiQS initiative through Grant GBMF6402, and by Rutgers University. G.S.T. thanks the Cluster of Excellence ct.qmat (Grant EXC2147) funded by the Deutsche Forschungsgemeinschaft for partial support at later stages of this work. The authors thank Michael B. Weissman, Philip W. Phillips, Lucas K. Wagner, Dale J. Van Harlingen, Zhenyu Wang, Michael Crommie, Nadya Mason, and Sander Otte for useful conversations.

Author affiliations: ^aDepartment of Physics, University of Illinois Urbana–Champaign, Urbana, IL 61801; ^bMaterials Research Laboratory, University of Illinois Urbana–Champaign, Urbana, IL 61801; ^cMax Planck Institute for Chemical Physics of Solids, 01187 Dresden, Germany; ^dFaculty of Chemistry and Food Chemistry, Technical University, 01069 Dresden, Germany; ^eLaboratory for Pohang Emergent Materials, Department of Physics, Pohang University of Science and Technology, Pohang 37673, Korea; ^eMax Plank Pohang University of Science and Technology (POSTECH) Center for Complex Phase Materials, Pohang University of Science and Technology, Pohang 37673, Korea; ^eRutgers Center for Emergent Materials, Rutgers University, Piscataway, NJ 08854; and ^hDepartment of Physics and Astronomy, Rutgers University, Piscataway,

- A. A. Khajetoorians et al., Atom-by-atom engineering and magnetometry of tailored nanomagnets. Nat. Phys. 8, 497–503 (2012).
- A. A. Khajetoorians et al., Current-driven spin dynamics of artificially constructed quantum magnets. Science 339, 55–59 (2013).
- W. Paul et al., Control of the millisecond spin lifetime of an electrically probed atom. Nat. Phys. 13, 403–407 (2017).
- F. D. Natterer et al., Reading and writing single-atom magnets. Nature 543, 226–228 (2017).
- S. Yan et al., Nonlocally sensing the magnetic states of nanoscale antiferromagnets with an atomic spin sensor. Sci. Adv. 3, e1603137 (2017).
- A. A. Khajetoorians, D. Wegner, A. F. Otte, I. Swart, Creating designer quantum states of matter atom-by-atom. *Nat. Rev. Phys.* 1, 703–715 (2019).
- J. Hermenau et al., Stabilizing spin systems via symmetrically tailored RKKY interactions. Nat. Commun. 10, 2565 (2019).
- E. C. Regan et al., Mott and generalized Wigner crystal states in WSe₂/WS₂ moiré superlattices. Nature 579, 359-363 (2020).

- F. J. Di Salvo, J. E. Graebner, The low temperature electrical properties of 1T-TaS₂. Solid State Commun. 23, 825-828 (1977).
- N. V. Smith, S. D. Kevan, F. J. DiSalvo, Band structures of the layer compounds 1T-TaS₂ and 2H-TaSe₂ in the presence of commensurate charge-density waves. *J. Phys. C Solid State Phys.* 18, 3175–3189 (1985).
- P. Fazekas, E. Tosatti, Electrical, structural and magnetic properties of pure and doped 1T-TaS₂. Philos. Mag. B Phys. Condens. Matter Electron. Opt. Magn. Prop. 39, 229-244 (1979).
- L. Perfetti, T. A. Gloor, F. Mila, H. Berger, M. Grioni, Unexpected periodicity in the quasi-twodimensional Mott insulator 1T-TaS₂ revealed by angle-resolved photoemission. *Phys. Rev. B Condens. Matter Mater. Phys.* 71, 153101 (2005).
- K. Rossnagel, N. V. Smith, Spin-orbit coupling in the band structure of reconstructed 1T-TaS₂. Phys. Rev. B Condens. Matter Mater. Phys. 73, 73106 (2006).
- 22. K. T. Law, P. A. Lee, 1T-TaS₂ as a quantum spin liquid. *Proc. Natl. Acad. Sci. U.S.A.* **114**, 6996–7000 (2017).
- W. Ruan et al., Evidence for quantum spin liquid behaviour in single-layer 1T-TaSe₂ from scanning tunnelling microscopy. Nat. Phys. 17, 1154–1161 (2021).

- L. Ma et al., A metallic mosaic phase and the origin of Mott-insulating state in 1T-TaS₂. Nat. Commun. 7, 10956 (2016).
 D. Cho et al., Correlated electronic states at domain walls of a Mott-charge-density-wave insulator
- D. Cho et al., Correlated electronic states at domain walls of a Mott-charge-density-wave insulato 1T-TaS₂. Nat. Commun. 8, 392 (2017).
- J. Skolimowski, Y. Gerasimenko, R. Žitko, Mottness collapse without metallization in the domain wall of the triangular-lattice Mott insulator 1T-TaS_2. Phys. Rev. Lett. 122, 036802 (2019)
- S. Qiao et al., Mottness collapse in 1T-TaS_{2-x}Se_x transition-metal dichalcogenide: An interplay between localized and itinerant orbitals. Phys. Rev. X7, 41054 (2017).
- D. Cho et al., Nanoscale manipulation of the Mott insulating state coupled to charge order in 1T-TaS₂. Nat. Commun. 7, 10453 (2016).
- R. Toskovic et al., Atomic spin-chain realization of a model for quantum criticality. Nat. Phys. 12, 656-660 (2016).
- S. Rolf-Pissarczyk et al., Dynamical negative differential resistance in antiferromagnetically coupled few-atom spin chains. Phys. Rev. Lett. 119, 217201 (2017).